

# Alterations in SCAI Expression during Cell Plasticity, Fibrosis and Cancer

Ákos Gasparics<sup>1</sup> · Gábor Kökény<sup>1</sup> · Attila Fintha<sup>2</sup> · Rita Bencs<sup>1</sup> · Miklós M. Mózes<sup>1</sup> · Emese Irma Ágoston<sup>3</sup> · Anna Buday<sup>1</sup> · Zoltán Ivics<sup>4</sup> · Péter Hamar<sup>1</sup> · Balázs Gyórfy<sup>5,6</sup> · László Rosivall<sup>1</sup> · Attila Sebe<sup>1,4</sup> 

Received: 20 June 2017 / Accepted: 9 August 2017 / Published online: 16 August 2017  
© Arányi Lajos Foundation 2017

**Abstract** Suppressor of cancer cell invasion (SCAI) has been originally characterized as a tumor suppressor inhibiting metastasis in different human cancer cells, and it has been suggested that SCAI expression declines in tumors. The expression patterns and role of SCAI during physiological and pathophysiological processes is still poorly understood. Earlier we demonstrated that SCAI is regulating the epithelial-mesenchymal transition of proximal tubular epithelial cells, it is downregulated during renal fibrosis and it is overexpressed in Wilms' tumors. Here we bring further evidence for the involvement of SCAI during cell plasticity and we examine the prognostic value and expression patterns of SCAI in various tumors. SCAI prevented the activation of the SMA promoter induced by angiotensin II. SCAI expression decreased in a model of endothelial-mesenchymal transition and increased during iPS reprogramming of fibroblasts. During renal fibrosis SCAI expression declined, as evidenced in a rat model of renal transplant rejection and in TGF- $\beta$ 1 overexpressing transgenic mice.

High expression of SCAI correlated with better survival in patients with breast and lung cancers. Intriguingly, in the case of other cancers (gastric, prostate, colorectal) high SCAI expression correlated with poor survival of patients. Finally, we bring evidence for SCAI overexpression in colorectal cancer patients, irrespective of stage or metastatic status of the disease, suggesting a diverse role of SCAI in various diseases and cancer.

**Keywords** Suppressor of cancer cell invasion (SCAI) · Epithelial-mesenchymal transition (EMT) · Cell plasticity · Fibrosis · Cancer

## Introduction

SCAI (Suppressor of Cancer Cell Invasion) is a relatively recently characterized interacting partner of Myocardin Related Transcription Factor/Serum Response Factor (MRTF/SRF). Consistent with the role of MRTFs in tumor progression and epithelial-mesenchymal transition (EMT) [1–3], SCAI acts through the transcriptional repression of the MKL-SRF complex [4], and as such, through the inhibition of CArG dependent gene expression [5]. Consistent with a tumor suppressor role, SCAI inhibits tumor cell invasion,  $\beta$ <sub>1</sub>-integrin expression [4] and EMT [5]. The role of SCAI during EMT is well established, SCAI regulates the expression of several markers and regulators of EMT. It inhibits TGF- $\beta$ 1 induced expression of CTGF, calponin and SMA. It also prevents TGF- $\beta$ 1 induced E-cadherin downregulation, through regulating Snail expression [6]. SCAI directly regulates TWIST expression, and SCAI downregulation led to transcriptional activation of the Wnt/ $\beta$ -catenin pathway [6]. SCAI controls gene expression by the interaction with the SWI/SNF complex and SWI/SNF could be a downstream mediator for SCAI signaling [7]. MRTF also contributes to dendritic

✉ Attila Sebe  
sebe.attila@med.semmelweis-univ.hu

<sup>1</sup> Department of Pathophysiology, Semmelweis University, Nagyvarad ter 4, rm 1810, Budapest 1089, Hungary

<sup>2</sup> 2nd Department of Pathology, Semmelweis University, Budapest, Hungary

<sup>3</sup> 1st Department of Surgery, Semmelweis University, Budapest, Hungary

<sup>4</sup> Division of Medical Biotechnology, Paul Ehrlich Institute, Langen, Germany

<sup>5</sup> MTA TTK Lendület Cancer Biomarker Research Group, Budapest, Hungary

<sup>6</sup> 2nd Department of Pediatrics, Semmelweis University, Budapest, Hungary

complexity of rat cortical neurons, and as an inhibitory cofactor of MRTF, overexpression of SCAI blocks SRF-dependent transcriptional responses and dendritic complexity [8].

SCAI is expressed in epithelial cells, where it shows a predominantly nuclear expression. Myofibroblasts present lower SCAI expression in response to TGF- $\beta$ 1 signaling [5]. Generally, reduced SCAI expression was found in several tumors [4, 6]. However, it seems that a downregulation of SCAI does not occur in all types of cancer: Wilms' tumors show very high expression of SCAI [5].

Here we further investigated the potential roles of SCAI during renal fibrosis and cancer focusing on SCAI dependent signaling mechanisms, SCAI expression patterns and prognostic value. Similarly to TGF- $\beta$ 1, angiotensin II is also known to mediate EMT in renal proximal tubular epithelial cells shown in the rat NRK-52E cell line [9]. We show here that angiotensin II mediated activation of the SMA promoter can be inhibited by SCAI overexpression. Higher SCAI expression is linked to the epithelial phenotype during reprogramming of fibroblasts to induced pluripotent stem cells (iPSC), a model that mimics a mesenchymal-to-epithelial transition-like (MET) process [10, 11]. Further, stimulation of endothelial cells with activated tumor cell conditioned medium to induce an endothelial-mesenchymal transition (EndMT) caused a reduction of SCAI expression. In the present study SCAI was downregulated in the kidneys of TGF- $\beta$ 1 transgenic mice and SCAI expression declined during renal transplant rejection. In the setting of cancer we bring evidence that, in contrary to other tumors, SCAI is highly overexpressed in colorectal cancers, and high SCAI expression levels correlate with poor colorectal cancer patient survival.

Our data bring further evidence to link SCAI to cell plasticity. Certain aspects of SCAI expression patterns during pathological conditions are in concordance with earlier findings. Interestingly, conflicting patient survival data and prognostic value of SCAI was found in different cancers. Surprisingly, SCAI was overexpressed in colorectal cancers, underlining the need to further investigate the exact role and function of SCAI during health and disease progression.

## Materials and Methods

### Cell Culture and Treatments

For experiments cells were grown on 6-well plates at 37 °C under a humidified atmosphere containing 5% CO<sub>2</sub>, and subjected to various treatments.

LLC-PK1 (CL4) proximal tubular epithelial cells were cultured in Dulbecco's modified Eagle's medium (Invitrogen, Carlsbad, CA), supplemented with 10% fetal bovine serum (FBS, Invitrogen) and 1% penicillin-streptomycin. Angiotensin II (Sigma-Aldrich, St. Louis, MO) treatments were performed as specified at the individual experiments (10<sup>-7</sup> M or vehicle for

controls). For inhibitor studies, cells were preincubated with 10<sup>-7</sup> M candesartan (Astra Zeneca, Mölndal, Sweden) or 10  $\mu$ mol/L CCG-1423 (Merck Chemicals, Darmstadt, Germany), a specific inhibitor of MRTF dependent signaling [12], for one hour.

Human umbilical vein endothelial cells (HUVECs) were isolated as described previously [13, 14]. Cells were grown on 0.5% gelatin-coated flasks (Sigma) and cultured in M199 medium (Sigma) supplemented with 15% FBS (Life Technologies), 100 IU/ml penicillin (Life Technologies), 100  $\mu$ g/ml streptomycin (Life Technologies), 7.5 IU/ml heparin (Merckle, Ulm, Germany), 2 ng/ml epidermal growth factor (R&D Systems, Abington, UK), and 250 pg/ml  $\beta$ -endothelial cell growth factor (R&D Systems), referred to as complete medium. Cells from passages 2–4 were used for experiments.

B16/F10 murine melanoma cells were kept in RPMI medium (Sigma) supplemented with 5% FBS (Life Technologies) and Glutamax (Life Technologies).

To obtain cancer cell line conditioned medium for HUVECs, serum-free M199 medium was collected after 24 h from B16/F10 cells. Latent TGF- $\beta$  was heat activated (80 °C, 10 min). FBS was supplemented before adding non-activated or activated conditioned medium to HUVECs.

Human iPS cells were reprogrammed as described previously [15, 16]. Three established iPS clones were grown on Matrigel (Corning Incorporated Life Sciences, Tewksbury, MA, USA) coated 6-well plates in mTeSR1 medium (Stem Cell Technologies).

### Plasmids

The PA3-Luc vector containing a 765-bp fragment of the rat SMA promoter (pSMA-Luc) was a kind gift from Dr. Raphael Nemenoff (University of Colorado, Denver, CO). The thymidine kinase-driven Renilla luciferase vector (pRL-TK), used as an internal control for transfection efficiency, was obtained from Promega (Madison, WI).

Green fluorescent protein (GFP)-tagged wild-type SCAI (GFP-SCAI) was obtained from Dr. Robert Grosse (University of Heidelberg, Heidelberg, Germany) and was previously described [4]. The dominant negative truncation mutant ( $\Delta$ C585) of myocardin (DN MyoC) known to inhibit MRTFs as well as kindly provided Dr. Eric N. Olson (University of Texas, Dallas, TX) and was previously described [17].

### Luciferase Assays

Luciferase assays were performed as earlier [5]. Briefly, cells were transfected with FuGene6 (Promega) and 0.5  $\mu$ g promoter construct, 0.05  $\mu$ g pRL-TK, and 2  $\mu$ g of either empty vector (pcDNA3.1) or the specific construct to be tested. For each measurement point three parallel wells were transfected. Firefly and Renilla luciferase activities were measured by

the Dual-Luciferase Reporter Assay Kit (Promega) according to the manufacturer's instructions. Results were normalized by dividing the Firefly luciferase activity with the Renilla luciferase activity of the same sample. Experiments were repeated at least three times. Results are presented as mean  $\pm$  SE.

### Kidney Transplant Rejection Model

Male Lewis (LEW, RT1<sup>l</sup>) and Brown-Norway (BN, RT1<sup>n</sup>) rats were obtained from Charles River (Munich, Germany, through Akrom Kft., Budapest, Hungary). Lewis-Brown-Norway (LEW x BN F1, LBN) hybrid rats were bred at the animal facility of Semmelweis University. LBN rats served as donors and LEW rats as recipients of kidney grafts. Rats at 8 weeks of age were used throughout the experiment. The rats were housed under standard conditions, and received rat chow and water ad libitum. All experimental procedures were in accordance with the Guide for the Care and Use of Laboratory Animals published by the US National Institutes of Health. The experimental protocol was reviewed and approved by the "Institutional Ethical Committee for Animal Care and Use" of Semmelweis University Budapest, Hungary (XIV-I-001/2012–4/2012).

LBN rats served as donors and Lewis rats as recipients. Animals were anesthetized with Pentobarbital-sodium 60 mg/kg (Euthasol 40%, Produlab Pharma, Raamsdonksveer, The Netherlands). Transplantation was performed as previously described [18, 19]. LBN-to-Lewis (LBN-to-LEW) rat kidney allografts were investigated. Non-transplanted native right kidneys of LBN rats (donors) were included as controls. Briefly, the left renal vessels of the donor were isolated and clamped. The donor kidney was perfused with 4 °C cold transplant buffer solution, removed, and positioned orthotopically into the recipient, whose renal vessels had been isolated, clamped, and the left native kidney removed. End-to-end anastomosis of renal artery, vein, and ureter was performed using 10–0 prolene sutures. Total graft ischemia was set to 30 min. No immunosuppression was applied. Postoperative care included morphine hydrochloride (Buprenorphine, Alstoe Limited, Sherriff Hutton, York, UK, 2.5 mg/kg s.c. after the operation) analgesia and ceftriaxone (Rocephine) 25 mg/kg i.p. once after operation, sc. (Roche Hungary Ltd., Budaörs, Hungary) to prevent infectious complications. On the second postoperative day the right native kidney was removed. Body weight was measured urine was collected and blood was taken from the tail vein daily after right nephrectomy. Serum and urine samples were stored at –80 °C for later measurements. Under isoflurane narcosis rats were exsanguinated from the abdominal aorta and were perfused with physiologic salt solution transcardially. Kidney grafts were removed and pieces were snap frozen in liquid nitrogen and stored at –80 °C for later western blot analysis. Experiments were terminated on the 4th and 7th postoperative day.

### Western Blot

Kidney tissues were homogenized into 200  $\mu$ l RIPA buffer using a tissue glass Dounce homogenizer. Protein concentration was determined using the BCA Protein Assay (Pierce Thermo Scientific, Rockford, USA). Samples were diluted into RIPA buffer and 20  $\mu$ g were loaded for Western blot. Western blots were carried out as described previously [5] using the following antibodies purchased from Sigma: anti-SCAI, anti- $\alpha$ -SMA, anti- $\alpha$ -tubulin.

### TGF- $\beta$ Transgenic Mice

CBA.B6-Alb/TGF- $\beta$ 1(cys223,225ser) transgenic mice were kindly provided by Dr. S.S. Thorgeirsson [20] and were maintained with continuous backcrosses to CBAXB6 F1 females. Mice were housed under specific pathogen free conditions (Semmelweis University NET GMO facility) with a 10/14 h light/dark cycle. Mice had access to rodent chow and drinking water ad libitum. All animal experiments were approved by the Semmelweis University Ethical Committee for Animal Welfare (XIV-I-001/2146–4/2012) and adhered to the NIH Guidelines for the Care and Use of Laboratory Animals.

### RT-qPCR Analysis of SCAI mRNA Expression

For quantitative RT-PCR experiments in kidneys of TGF- $\beta$  transgenic mice 100 mg of whole kidneys were homogenized and total RNA was isolated according to the manufacturer's protocol (SV Total RNA Kit, Promega, Madison, WI, USA). 2  $\mu$ g RNA was reverse transcribed (High Capacity cDNA Reverse Transcription Kit, Applied Biosystems, Foster City, CA, USA) using random primers. PCR reactions were performed on a BioRad CFX thermocycler (BioRad, Hercules, CA, USA) using the Maxima SYBR Green PCR Master Mix (Thermo) and 95 °C for 15 s and 60 °C for 60 s for 40 cycles. Specificity and efficiency of the PCR reaction was confirmed with melting curve and standard curve analysis, respectively. Mean values are expressed with the formula  $2^{-\Delta\Delta Ct}$ .

When analyzing SCAI mRNA expression in HUVEC and iPS cells, cells were washed once with PBS and total RNA was isolated using TRIzol (Invitrogen), following the instructions of the manufacturer. Reverse transcription and RT-PCR were performed as above. Three parallels were measured for each experimental point, and the experiment was repeated two times.

Primer sequences were as follows: mSCAI forward: acccctgttcacgttg, mSCAI reverse: cgagtgctgtccaaaca, mGAPDH forward: cttgtcaagctcattctgg, mGAPDH reverse: tcttctcagtgctcttgc, hSCAI forward: cggaacacgaaattacc, hSCAI reverse: gcttctggagatgaggattctc, hE-cadherin forward: ggctggaccgagagagttc, hE-cadherin reverse: cctgacctgtacgtggtg, hNanog forward: acctcagctacaacaggtgaag, hNanog reverse: agagtaaaggctgggtaggt, hGAPDH forward: cccttcattgacctcaacta;

hGAPDH reverse: ccaaagttgtcatggatgac, h18S forward: ccccatgaacgaggggaatt, h18S reverse: gggactaatcaacgcaagctt.

### Database Setup for Patient Survival Analysis

Gene expression datasets for breast and lung cancer patients were established as described previously [21, 22]. Databases for gastric, colon, and prostate cancers were established following way: gene expression data was identified in GEO (<http://www.ncbi.nlm.nih.gov/geo/>). In this, the keywords “tumor tissue of origin”, “cancer”, “gpl96”, “gpl571” and “gpl570” were used. Only publications with available raw data, clinical survival information, and at least 30 patients were included. Only Affymetrix HG-U133A (GPL96), HG-U133Aplus2 (GPL571) and HG-U133 Plus 2.0 (GPL570) gene chips were considered, because they are frequently used and because these particular chips measure the expression for a set of genes using the exact same probe sets.

For statistical analysis the raw CEL files were MAS5 normalized in the R statistical environment ([www.r-project.org](http://www.r-project.org)) using the affy Bioconductor library. We selected MAS5 because it ranked among the best normalization methods when compared to the results of RT-PCR measurements in a previous study [23]. Then, only probes measured on each of the three array platforms were retained ( $n = 22,277$ ) and we performed a second scaling normalization to set the average expression on each chip to 1000 to avoid batch effects. Cox proportional hazard regression was utilized for survival analysis. Kaplan-Meier survival plot and the hazard ratio with 95% confidence intervals and logrank  $P$  value were calculated and plotted in R as described previously [24]. Statistical significance was set at  $p < 0.05$ .

### Gene Microarray Data Analysis

For this, sets of gene expression profiles were downloaded from Gene Expression Omnibus (GEO) of the National Center for Biotechnology Information (NCBI). SCAI gene expression levels were compared in three different datasets: breast cancer (GDS3853, healthy breast tissue, ductal carcinoma in situ, invasive ductal carcinoma), colorectal cancer (GSE21815, healthy tissue, colorectal cancer stages 1–4), metastatic colorectal cancer (GDS4393, primary lesions, metastatic lesions).

### Immunohistochemical Analysis of Human Colorectal Cancer Samples

Samples were retrieved from the archives of the 2nd Department of Pathology, Semmelweis University, according to the approval of the local Institutional Review Board (IKEB #207/2011). Formalin-fixed, paraffin-embedded (FFPE)

samples were used for tissue microarrays. Eight 1 mm cores were analyzed from each sample. Normal colon mucosa and main tumor mass areas were selected from all resection specimens. Staining was carried out as described earlier [5]. Digital imaging of immunostained specimens was performed using a Panoramic P250beta slide scanner with 40× objective and a Hitachi camera (3DHistech Ltd., Budapest, Hungary). SCAI expression patterns were analyzed using the NuclearQuant modul of the 3DHistech Panoramic Viewer. H-score was calculated by classifying staining intensity as follows: 0: none, 1: weak, 2: intermediate, 3: strong expression.

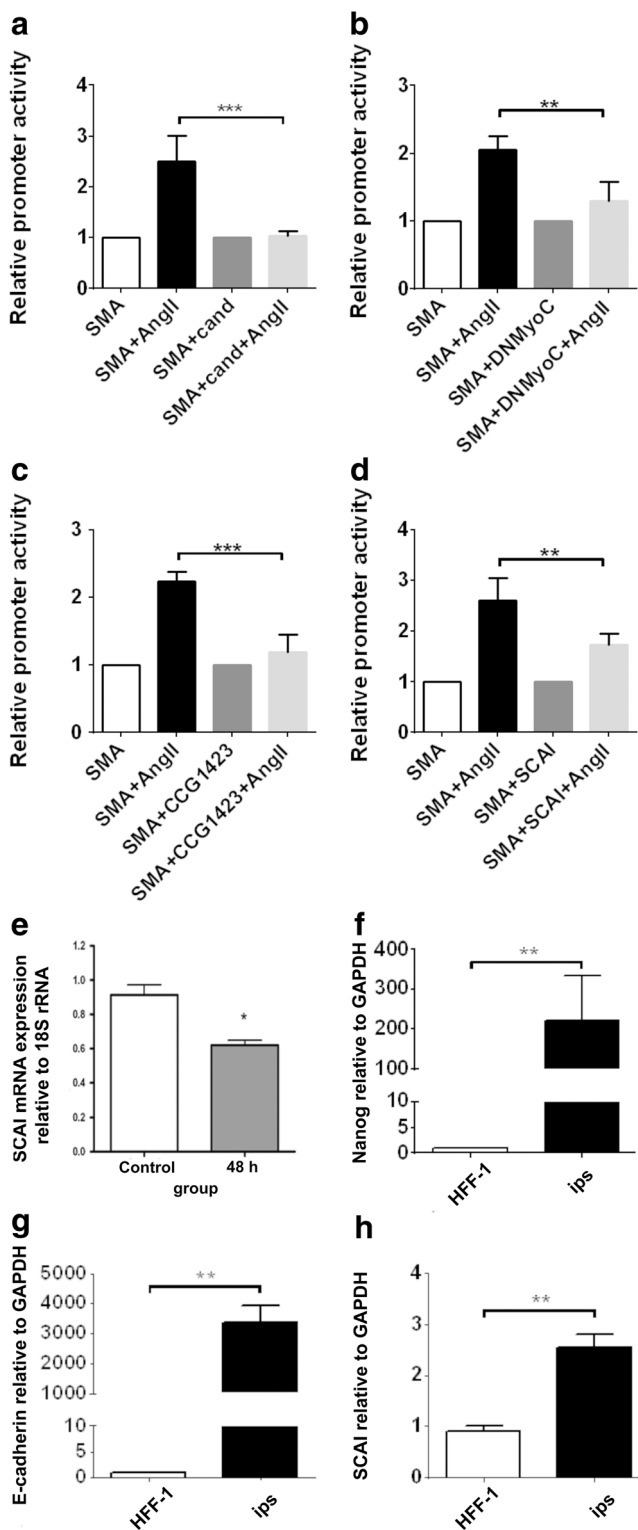
## Results

### 1. SCAI Expression during Cell Plasticity

First, to validate earlier findings in our EMT model established on LLC-PK1 porcine renal proximal tubular epithelial cells, LLC-PK1 cells were transfected with the SMA promoter and were treated with angiotensin II. Angiotensin II induced SMA promoter activation and this effect was mitigated in the presence of candesartan, a specific inhibitor of AT<sub>1</sub> receptor (Fig. 1a). To test whether angiotensin II dependent SMA promoter activation is mediated through MRTFs, two experiments were designed. Co-transfection of a dominant negative form of MyoC known to inhibit MRTFs diminished the effects of angiotensin II on the SMA promoter (Fig. 1b). Similarly, CCG-1423, a specific inhibitor of MRTF dependent signaling, prevented angiotensin II induced SMA promoter activation (Fig. 1c). Based on this data we concluded that MRTFs mediate angiotensin II dependent SMA promoter activation. When SCAI was co-transfected along the SMA promoter, it prevented the effects of angiotensin II stimulation (Fig. 1d). SCAI is therefore preventing SMA promoter activation upon both angiotensin II and TGF- $\beta$ 1 stimulation.

Earlier we linked higher levels of SCAI expression to an epithelial phenotype in the context of EMT [5]. Activated tumor cell conditioned medium can induce a TGF- $\beta$ 1 mediated endothelial-mesenchymal transition in HUVECs and cerebral endothelial cells, a phenomenon which could be important during metastatic extravasation [14]. In accordance with previous observations, treatment of HUVEC cells with activated tumor cell conditioned medium lead to a significant decrease in SCAI mRNA levels (Fig. 1e).

Reprogramming fibroblasts into iPS cells represents a powerful tool to investigate mesenchymal-to-epithelial transition. To validate our findings on its expression changes during EMT, SCAI expression was followed in fibroblasts and in their iPSC derivate. As expected, in parallel to acquiring stemness characterized by Nanog (Fig. 1f) and E-cadherin (Fig. 1g) expression, cells undergoing iPSC reprogramming



exhibited a significant and dramatic increase in SCAI expression as well (Fig. 1h). This data supports the hypothesis that higher SCAI expression is likely more linked to an epithelial/endothelial phenotype, and it is expressed less in mesenchymal and mesenchymal-like cells.

**Fig. 1** Linking SCAI and cell plasticity. **a** The AT1 receptor inhibitor candesartan inhibited angiotensin II induced SMA promoter activation in luciferase assays. Cells were transfected with SMA promoter and treated with angiotensin II. Pretreatment of cells with candesartan inhibited the effect of angiotensin II ( $2.5 \pm 0.5$  vs.  $1.02 \pm 0.09$ ,  $*** p < 0.001$ , Mann-Whitney U-test). **b** Inhibition of MRTFs reduced angiotensin II induced activation of the SMA promoter in luciferase assays. Cells were transfected with SMA promoter with or without DNMyoC and were treated with angiotensin II. DNMyoC reduced the activation of the SMA promoter induced by angiotensin II ( $2.05 \pm 0.2$  vs.  $1.29 \pm 0.29$ ,  $** p < 0.01$ , Mann-Whitney U-test). **c** CCG1423, a specific inhibitor of MRTF signaling, prevented angiotensin II induced activation of the SMA promoter in luciferase assays. Cells were transfected with SMA promoter and treated with angiotensin II. Pretreatment of cells with candesartan inhibited the effect of angiotensin II ( $2.23 \pm 0.15$  vs.  $1.19 \pm 0.25$ ,  $*** p < 0.001$ , Mann-Whitney U-test). **d** SCAI reduced angiotensin II induced SMA promoter activation, as shown by luciferase assays. Cells were transfected with SMA promoter with or without SCAI and were treated with angiotensin II. SCAI reduced the activation of the SMA promoter induced by angiotensin II ( $2.6 \pm 0.43$  vs.  $1.72 \pm 0.22$ ,  $** p < 0.01$ , Mann-Whitney U-test). **e** SCAI mRNA expression decreases in a model of endothelial- mesenchymal transition. HUVECs were incubated in activated tumor cell conditioned medium for 48 h and mRNA was examined. SCAI mRNA levels significantly decreased in stimulated HUVECs as compared to HUVECs grown under control conditions ( $* p < 0.05$ , Mann-Whitney U-test). **f, g, h** Reprogramming of fibroblasts to iPS cells corresponds in many aspects to a mesenchymal-to-epithelial transition. Fibroblasts are negative for E-cadherin and Nanog. In parallel with a massive overexpression of E-cadherin (F) and Nanog (G) mRNA, iPS reprogramming results in the significant overexpression of SCAI mRNA as well (H). Three iPS clones were examined and mRNA expression was compared to parental HFF-1 fibroblasts ( $** p < 0.01$ , Mann-Whitney U-test)

## 2. SCAI Expression is Reduced in Fibrotic Kidneys

Earlier, SCAI expression was shown to be decreased in a rat diabetic nephropathy model and in human fibrotic kidneys. Another challenging aspect in the field of nephrology and fibrotic renal disease is chronic interstitial fibrosis and tubular atrophy (IF/TA) the main cause of late allograft loss. One important mechanism involved in this process is EMT [25]. We investigated if SCAI expression would change during early fibrotic events occurring in allograft nephropathy. For this we used the LBNF1-to-LEW rat kidney allograft rejection model leading to IF/TA [26]. We examined the allografts 4 and 7 days post transplantation to observe the very early events of IF/TA development. Right kidneys of transplanted Lewis rats were used as controls. In parallel with an increase in SMA protein expression rejecting kidneys exhibited a steep decrease of SCAI protein expression already 4 days after transplantation, and more pronounced on day 7 (Fig. 2a).

In vitro experimental observations indicated that TGF- $\beta$ 1 is one of the inducers of SCAI expressional decline. Here we present in vivo evidence linking SCAI expression to TGF- $\beta$ 1 mediated effects. For this we assessed SCAI mRNA levels in the kidneys of a transgenic TGF- $\beta$ 1 overexpressing mouse strain, as compared to wild-type mouse kidneys. SCAI

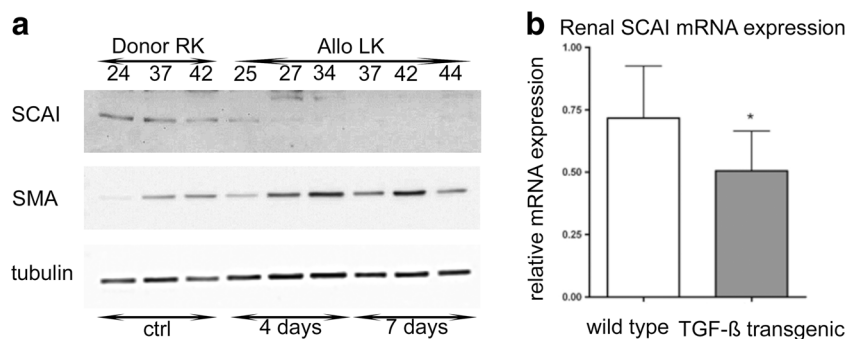


**Fig. 2** SCAI expression in kidneys. **a** SCAI protein expression was assessed in a LBNF1-to-LEW rat kidney allograft rejection model. Left kidney allografts at 4 and 7 days post transplantation were examined and compared to right kidneys of transplanted Lewis rats as controls. Western blot analysis of kidney tissues revealed that in parallel with the increase in

SMA expression SCAI expression suffered a steep decrease in the rejected kidneys. **b** SCAI mRNA levels in the kidneys of a transgenic TGF-β1 overexpressing mice were compared to wild-type mouse kidneys. SCAI mRNA was significantly downregulated in kidney of 14 days old TGF-β1 transgenic mice (\*  $p < 0.05$ , Mann-Whitney U-test)

mRNA was significantly downregulated in kidneys of TGF-β1 transgenic mice (Fig. 2b).

### 3. SCAI Prognostic Value and Expression in Cancer

We also assessed the prognostic value of SCAI in different cancers. For this hazard ratios were calculated and Kaplan-Meier plots were generated using large databases. Strikingly, for certain cancers (breast or lung cancer) the hazard ratio was  $< 1$  corresponding to a lower risk, other cancers (gastric, prostate, colon) had a hazard ratio  $> 1$  correlating with increased risk (Table 1). Concordantly, high expression of SCAI correlated with better survival in patients with breast and lung cancers (or their subgroups) (Fig. 3a-e), whereas in the case of another group of cancers (gastric, prostate, colorectal) high SCAI expression correlated with decreased survival of patients (Fig. 3f-j).

Focusing on breast and colorectal cancers publicly available databases were searched to compare SCAI expression levels in healthy and cancerous tissues. SCAI expression decreased in ductal carcinoma in situ and in invasive ductal

carcinoma, as compared to healthy breast tissue (Fig. 4a). In contrast to these observations, SCAI expression increased in colorectal cancers as compared to healthy colon tissue, irrespective of tumor stage: one publicly available expression database revealed that SCAI expression was more significant in stages 1–4 of colorectal cancer than in healthy colon tissue (Fig. 4b). Moreover, there was no significant difference in SCAI expression when primary colorectal cancer and metastatic tissue were compared as evidenced in data from another publicly available database (Fig. 4c).

To bring further evidence to survival data and SCAI expression levels in databases, we examined 9 colorectal cancers (Table 2) by immunohistochemistry and SCAI expression was scored. Immunohistochemistry also evidenced that the relatively low SCAI expression in healthy colon tissue became more pronounced in the tumor tissue (Fig. 4d). H scoring also evidenced the marked increase of SCAI staining in colorectal cancer tissues as compared to the staining in normal colon mucosa (Table 2).

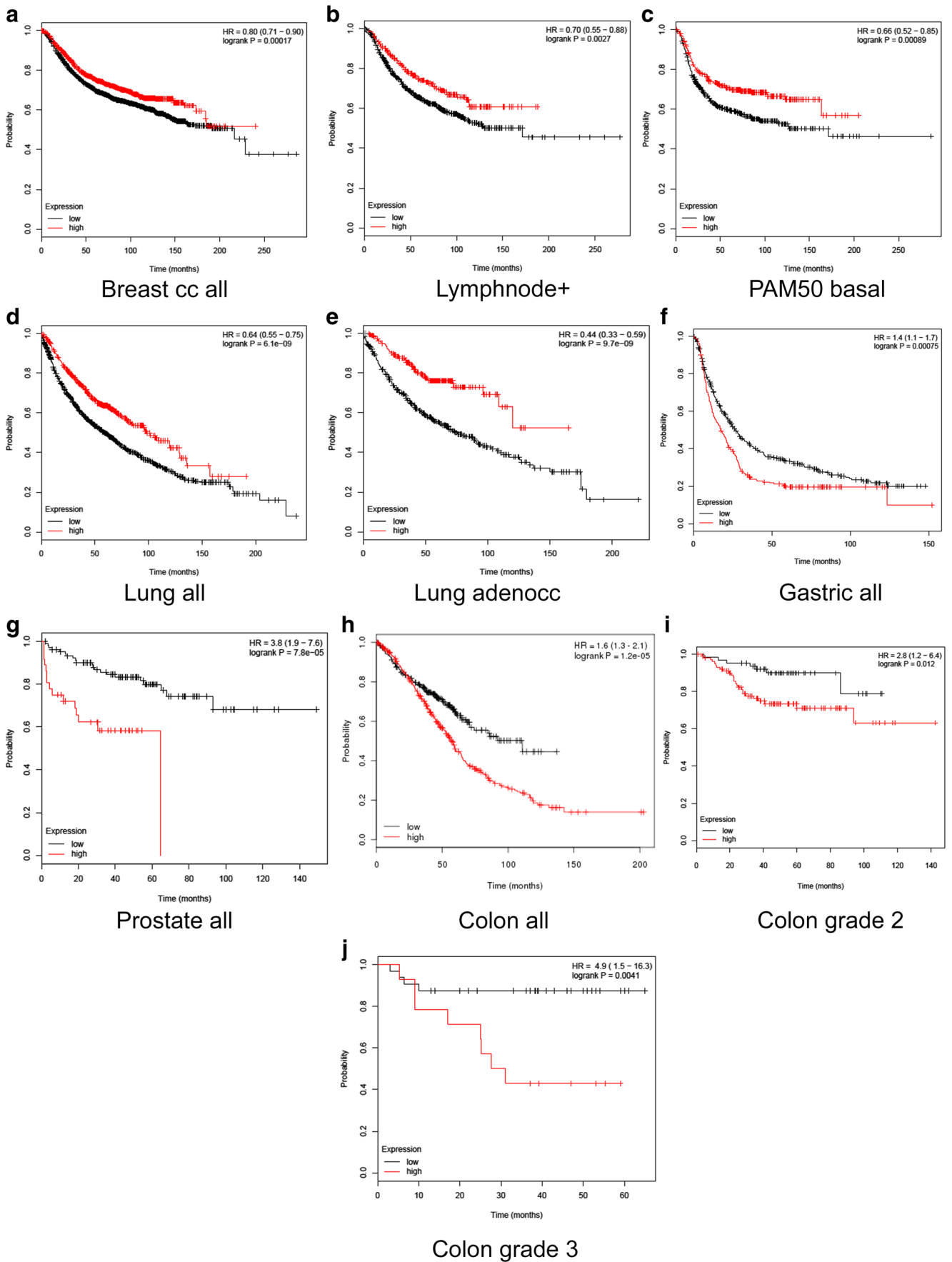
**Table 1** Hazard ratio (HR) in different tumors

Tumor location	Tumor subtype	HR	<i>P</i> value	Number of patients included in analysis
Breast	All	0.8	0.00017	3729
	Lymph node+	0.7	0.0027	1041
	PAM50 basal	0.66	0.00089	410
Lung	All	0.64	6.1E-09	1919
	Adenocarcinoma	0.44	9.7E-09	718
Gastric		1.75	1.40E-10	876
Prostate		3.8	0.000078	140
Colon	All	1.6	1.20E-05	813
	Grade 2	2.8	0.012	165
	Grade 3	4.9	0.0041	46

### Discussion

SCAI has been implicated in cell plasticity and EMT. SCAI was shown to interfere with TGF-β1-induced expression of EMT markers; moreover, it rescued TGF-β1-induced E-cadherin down-regulation [5], a finding in line with

**Fig. 3** Prognostic value of SCAI in different cancers. Kaplan-Meier plots were generated using large databases. High expression of SCAI correlated with better survival in patients with breast and lung cancers or their subgroups (**a** breast cancers, **b** lymph node positive breast cancers, **c** PAM50 basal breast cancers, **d** lung cancers, **e** lung adenocarcinomas), whereas in the case of another group of cancers (gastric, prostate, colorectal) high SCAI expression correlated with poor survival of patients (**f** gastric cancers, **g** prostate cancers, **h** colorectal cancers, **i** grade 2 colorectal cancers, **j** grade 3 colorectal cancers). Hazard ratios calculated based on these data are presented in Table 1



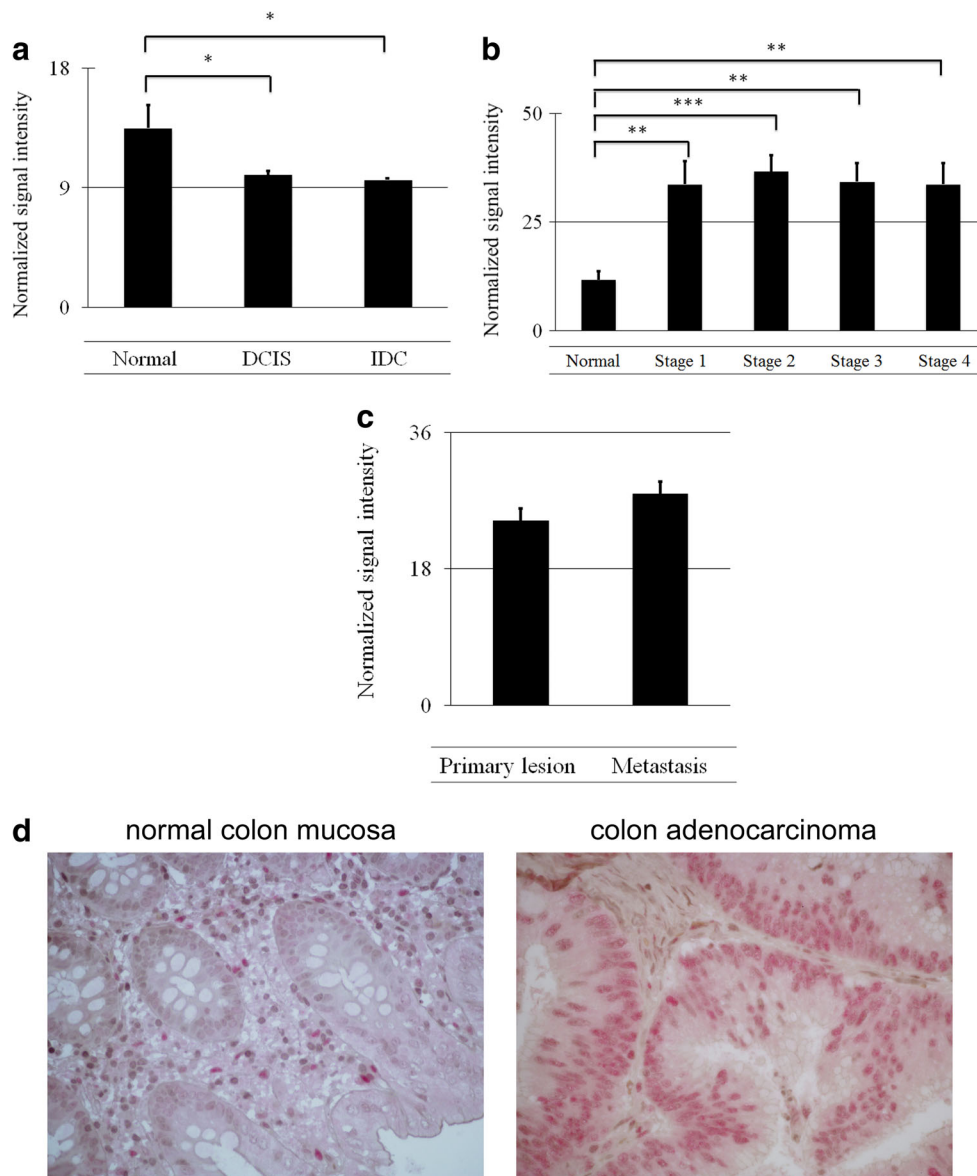


**Fig. 4** SCAI expression in human cancer tissues. **a** SCAI gene expression was compared in a breast cancer gene expression dataset (GDS3853): healthy breast tissue (healthy,  $n = 5$ ), ductal carcinoma in situ (DCIS,  $n = 9$ ), invasive ductal carcinoma (IDC,  $n = 5$ ). SCAI expression significantly declined in breast cancers as compared to healthy breast tissue ( $* p < 0.05$ , Kruskal-Wallis with Dunn's multiple comparison test). **b** SCAI gene expression was compared in a colorectal cancer gene expression dataset (GSE21815): normal colon mucosa (normal,  $n = 9$ ), colorectal cancer stage 1 (stage 1,  $n = 13$ ), colorectal cancer stage 2 (stage 2,  $n = 26$ ), colorectal cancer stage 3 (stage 3,  $n = 17$ ), colorectal cancer stage 4 (stage 4,  $n = 10$ ). SCAI mRNA expression significantly increased in colorectal cancers as compared to normal colon

mucosa, irrespective of the stage of the disease ( $** p < 0.01$ ,  $*** p < 0.001$ , Kruskal-Wallis with Dunn's multiple comparison test). **c** SCAI gene expression was compared in a metastatic colorectal cancer gene expression dataset (GDS4393): primary lesions ( $n = 33$ ), metastatic lesions ( $n = 21$ ). There was no significant difference in SCAI mRNA expression levels between primary lesions and metastatic lesions of colorectal carcinoma patients. **d** SCAI expression in colorectal cancers, representative images of SCAI immunohistochemistry. SCAI was expressed in normal colon mucosa at lower levels, colon adenocarcinoma presented a high expression of SCAI. A H-score quantification of SCAI immunohistochemistry analysis of 9 colorectal cancer patient tissues is shown in Table 2

observations in glioma cells: SCAI downregulation activated Wnt/ $\beta$ -catenin signaling, and blockade of the Wnt/ $\beta$ -catenin pathway abrogated the effects of SCAI downregulation on glioma cell aggressiveness. Further, expression of key EMT regulators Snail and TWIST is also SCAI-regulated [6]. Here we demonstrated that angiotensin II induced SMA promoter

activation can be influenced by the presence of SCAI, similarly to influencing TGF- $\beta$ 1-dependent signaling.

Despite earlier controversies, EMT and epithelial plasticity are important mechanisms during renal fibrosis [27]. In this context we showed earlier that kidneys of diabetic rats and mice with unilateral ureteral obstruction depicted significant



**Table 2** H-scoring of SCAI immunohistochemistry analysis of 9 human colorectal carcinoma and adjacent healthy tissues

Patient	Gender	Age	Location of tumor	Grade	T	N	Dukes	MAC	K-RAS	MSI	Ave H score Normal	Ave H score Tumor
1	M	84	Coecum	2	3	0	B	B2	Mut12	0	1.33	31.83
2	F	74	Sigma	2	3	0	D	D	Mut12	0	0.10	4.64
3	F	59	Descendens	2	3	1	C	C2	WT	0	0.00	26.71
4	F	57	Flex.hepatica	3	3	0	B	B2	WT	1	0.40	16.37
5	M	73	Ascendens	2	3	0	B	B2	WT	0	1.20	11.40
6	F	66	Ascendens	3	3	2	D	D	WT	0	3.28	15.71
7	F	53	Coecum	2	3	2	C	C3	Mut12	0	2.82	29.19
8	F	67	Sigma	2	3	1	D	D	WT	0	4.70	67.61
9	F	75	Rectum	2	3	2	C	C3	WT	0	1.53	34.29

M: male; F: female; Mut12: mutation in codon 12; WT: wild type; Ave H score Normal: SCAI immunohistochemistry average H score value for normal tissue; Ave H score Tumor: SCAI immunohistochemistry average H score value for tumor tissue

loss of SCAI expression [5]. Here we bring further *in vivo* data on the alterations of SCAI expression during renal fibrosis. SCAI mRNA expression was diminished in kidneys of TGF- $\beta$ 1 transgenic mice, and SCAI protein expression dramatically decreased in a model of renal transplant rejection, findings in concordance with our earlier observations.

As for the context of cancer, the current understanding is that SCAI is downregulated in cancers and is a suppressor of tumor cell invasion [4]. In glioma cells SCAI also inhibited the self-renewal ability of tumor cells, suggesting a more complex role in suppressing cancer progression. Observations on human breast cancer tissue evidenced that SCAI is downregulated in breast cancer [7, 28]. Accordingly, when assessing its prognostic value in databases, decreased expression of SCAI correlated with poor survival of breast and lung cancer patients. However, a contradicting observation was made in other types of cancers (gastric, prostate, and colorectal) where low SCAI expression correlated with better survival. Interestingly, in publicly available expression databases we found that SCAI expression is increased in stage 1–4 colorectal cancers when compared to healthy tissue. Further, there was no significant difference between SCAI expression in primary colorectal tumors or metastatic foci. Immunohistochemical analysis of human colorectal cancer specimens also evidenced an increase in SCAI staining in primary tumors, as compared to healthy tissue. This is not the only observation of this kind, Wilms' tumors are also characterized by high levels of SCAI expression, whereas other types of kidney tumors express low levels of SCAI [5]. These observations could mean that SCAI expression during cancer development could vary depending on the cell type of origin of the tumors. Indeed, it is well known that certain proteins may have pleiotropic functions, for example Notch can be tumor suppressive or oncogenic depending on the cellular context [29]. The limited amount of data available so far indicates a more complex role of SCAI in the pathophysiology of human disease.

The cellular function of SCAI has been only partially elucidated. Its potential involvement in cell plasticity and metastasis

can be explained by a mechanism involving the inhibition of MRTF-SRF dependent signaling [4–6]. Yet other specific effects still need to be elucidated. For example SCAI was shown to interact with the tumor suppressing SWI/SNF chromatin remodeling complex [7]. SCAI also interacts with heterochromatin protein 1 (HP1, product of the CBX5 gene) [30], which functions primarily as a gene silencer. Intriguingly, SCAI was also found to interact with KDM3B, an H3K9me1/2 histone demethylase [31]. Interestingly, the amino acid sequence of SCAI contains a PIP box defined by the Q-x-[x]-I/L/V-x-[x]-F/Y/W/H-F/Y/W/H sequence [32], at positions 526–532, which is known to be found in many PCNA-interacting proteins. Proteins binding to PCNA via the PIP-box are mainly involved in DNA replication and chromatin assembly [33]. PCNA binds to several regulators of chromatin organization, for example HDAC1, which plays an important role in gene silencing [34], WSTF-SNF2H chromatin-remodeling complex, or human heterochromatin protein HP1 [35]. Complexing of SCAI with these proteins hint to a potentially wider role for SCAI in chromatin organization. In concordance to these observations and hypothesis, it has been evidenced that SCAI is also involved in double-strand break repair mechanisms [36]. Recent data indicated that SCAI facilitates the recruitment of BRCA1 to damage sites during homology-directed repair [37], a functional synergy possibly relevant in the context of EMT as well: similarly to SCAI, BRCA1 is also known to suppresses EMT [38].

The data obtained in this study clearly provide new evidence for the involvement of SCAI in regulating cell plasticity and EMT. SCAI expression declines during renal fibrosis, and may have a prognostic value for certain cancers. The study brings further evidence to show that there are tumors where SCAI is not downregulated as hypothesized before, moreover, the prognostic value of SCAI in different tumors is contradictory. Thus, further studies are needed to elucidate the exact roles of SCAI during physiological and pathophysiological mechanisms and to implicate SCAI or its regulators as therapeutic targets.

**Acknowledgments** We thank Dr. Marcell A. Szász for valuable discussions, and Erika Skláňitzné Samodai for technical assistance.

### Compliance with Ethical Standards

**Conflicts of Interest** The authors declare no conflicts of interest.

### References

- Medjkane S, Perez-Sanchez C, Gaggioli C, Sahai E, Treisman R (2009) Myocardin-related transcription factors and SRF are required for cytoskeletal dynamics and experimental metastasis. *Nat Cell Biol* 11(3):257–268. doi:10.1038/ncb1833
- Fan L, Sebe A, Peterfi Z, Masszi A, Thirone AC, Rotstein OD, Nakano H, McCulloch CA, Szaszi K, Mucsi I, Kapus A (2007) Cell contact-dependent regulation of epithelial-myofibroblast transition via the rho-rho kinase-phospho-myosin pathway. *Mol Biol Cell* 18(3):1083–1097. doi:10.1091/mbc.E06-07-0602
- Sebe A, Masszi A, Zulus M, Yeung T, Speight P, Rotstein OD, Nakano H, Mucsi I, Szaszi K, Kapus A (2008) Rac, PAK and p38 regulate cell contact-dependent nuclear translocation of myocardin-related transcription factor. *FEBS Lett* 582(2):291–298. doi:10.1016/j.febslet.2007.12.021
- Brandt DT, Baarlink C, Kitzing TM, Kremmer E, Ivaska J, Nollau P, Grosse R (2009) SCAI acts as a suppressor of cancer cell invasion through the transcriptional control of beta1-integrin. *Nat Cell Biol* 11(5):557–568. doi:10.1038/ncb1862
- Fintha A, Gasparics A, Fang L, Erdei Z, Hamar P, Mozes MM, Kokeny G, Rosivall L, Sebe A (2013) Characterization and role of SCAI during renal fibrosis and epithelial-to-mesenchymal transition. *Am J Pathol* 182(2):388–400. doi:10.1016/j.ajpath.2012.10.009
- Chen X, Hu W, Xie B, Gao H, Xu C, Chen J (2014) Downregulation of SCAI enhances glioma cell invasion and stem cell like phenotype by activating Wnt/beta-catenin signaling. *Biochem Biophys Res Commun* 448(2):206–211. doi:10.1016/j.bbrc.2014.04.098
- Kressner C, Nollau P, Grosse R, Brandt DT (2013) Functional interaction of SCAI with the SWI/SNF complex for transcription and tumor cell invasion. *PLoS One* 8(8):e69947. doi:10.1371/journal.pone.0069947
- Ishikawa M, Nishijima N, Shiota J, Sakagami H, Tsuchida K, Mizukoshi M, Fukuchi M, Tsuda M, Tabuchi A (2010) Involvement of the serum response factor coactivator megakaryoblastic leukemia (MKL) in the activin-regulated dendritic complexity of rat cortical neurons. *J Biol Chem* 285(43):32734–32743. doi:10.1074/jbc.M110.118745
- Burns WC, Velkoska E, Dean R, Burrell LM, Thomas MC (2010) Angiotensin II mediates epithelial-to-mesenchymal transformation in tubular cells by ANG 1-7/MAS-1-dependent pathways. *Am J Physiol Ren Physiol* 299(3):F585–F593. doi:10.1152/ajprenal.00538.2009
- Li R, Liang J, Ni S, Zhou T, Qing X, Li H, He W, Chen J, Li F, Zhuang Q, Qin B, Xu J, Li W, Yang J, Gan Y, Qin D, Feng S, Song H, Yang D, Zhang B, Zeng L, Lai L, Esteban MA, Pei D (2010) A mesenchymal-to-epithelial transition initiates and is required for the nuclear reprogramming of mouse fibroblasts. *Cell Stem Cell* 7(1):51–63. doi:10.1016/j.stem.2010.04.014
- Samavarchi-Tehrani P, Golipour A, David L, Sung HK, Beyer TA, Datti A, Woltjen K, Nagy A, Wrana JL (2010) Functional genomics reveals a BMP-driven mesenchymal-to-epithelial transition in the initiation of somatic cell reprogramming. *Cell Stem Cell* 7(1):64–77. doi:10.1016/j.stem.2010.04.015
- Evelyn CR, Wade SM, Wang Q, Wu M, Iniguez-Lluhi JA, Merajver SD, Neubig RR (2007) CCG-1423: a small-molecule inhibitor of RhoA transcriptional signaling. *Mol Cancer Ther* 6(8):2249–2260. doi:10.1158/1535-7163.MCT-06-0782
- Bodor C, Nagy JP, Vegh B, Nemeth A, Jenei A, MirzaHosseini S, Sebe A, Rosivall L (2012) Angiotensin II increases the permeability and PV-1 expression of endothelial cells. *Am J Physiol Cell Physiol* 302(1):C267–C276. doi:10.1152/ajpcell.00138.2011
- Krizbai IA, Gasparics A, Nagyoszi P, Fazakas C, Molnar J, Wilhelm I, Bencs R, Rosivall L, Sebe A (2015) Endothelial-mesenchymal transition of brain endothelial cells: possible role during metastatic extravasation. *PLoS One* 10(3):e0119655. doi:10.1371/journal.pone.0119655
- Grabundzija I, Wang J, Sebe A, Erdei Z, Kajdi R, Devaraj A, Steinemann D, Szuhai K, Stein U, Cantz T, Schambach A, Baum C, Izsvak Z, Sarkadi B, Ivics Z (2013) Sleeping beauty transposon-based system for cellular reprogramming and targeted gene insertion in induced pluripotent stem cells. *Nucleic Acids Res* 41(3):1829–1847. doi:10.1093/nar/gks1305
- Sebe A, Ivics Z (2016) Reprogramming of human fibroblasts to induced pluripotent stem cells with sleeping beauty transposon-based stable gene delivery. *Methods Mol Biol* 1400:419–427. doi:10.1007/978-1-4939-3372-3\_26
- Wang D, Chang PS, Wang Z, Sutherland L, Richardson JA, Small E, Krieg PA, Olson EN (2001) Activation of cardiac gene expression by myocardin, a transcriptional cofactor for serum response factor. *Cell* 105(7):851–862
- Hamar P, Liu S, Viklicky O, Szabo A, Muller V, Heemann U (2000) Cyclosporine a and azathioprine are equipotent in chronic kidney allograft rejection. *Transplantation* 69(7):1290–1295
- Hamar P, Liptak P, Heemann U, Ivanyi B (2005) Ultrastructural analysis of the fisher to Lewis rat model of chronic allograft nephropathy. *Transpl Int* : Official journal of the European Society for Organ Transplantation 18(7):863–870. doi:10.1111/j.1432-2277.2005.00146.x
- Sanderson N, Factor V, Nagy P, Kopp J, Kondaiah P, Wakefield L, Roberts AB, Sporn MB, Thorgeirsson SS (1995) Hepatic expression of mature transforming growth factor beta 1 in transgenic mice results in multiple tissue lesions. *Proc Natl Acad Sci U S A* 92(7):2572–2576
- Gyorffy B, Lanczky A, Eklund AC, Denkert C, Budczies J, Li Q, Szallasi Z (2010) An online survival analysis tool to rapidly assess the effect of 22,277 genes on breast cancer prognosis using microarray data of 1,809 patients. *Breast Cancer Res Treat* 123(3):725–731. doi:10.1007/s10549-009-0674-9
- Gyorffy B, Surowiak P, Budczies J, Lanczky A (2013) Online survival analysis software to assess the prognostic value of biomarkers using transcriptomic data in non-small-cell lung cancer. *PLoS One* 8(12):e82241. doi:10.1371/journal.pone.0082241
- Gyorffy B, Molnar B, Lage H, Szallasi Z, Eklund AC (2009) Evaluation of microarray preprocessing algorithms based on concordance with RT-PCR in clinical samples. *PLoS One* 4(5):e5645. doi:10.1371/journal.pone.0005645
- Mihaly Z, Kormos M, Lanczky A, Dank M, Budczies J, Szasz MA, Gyorffy B (2013) A meta-analysis of gene expression-based biomarkers predicting outcome after tamoxifen treatment in breast cancer. *Breast Cancer Res Treat* 140(2):219–232. doi:10.1007/s10549-013-2622-y
- Li X, Zhuang S (2014) Recent advances in renal interstitial fibrosis and tubular atrophy after kidney transplantation. *Fibrogenesis Tissue Repair* 7:15. doi:10.1186/1755-1536-7-15
- Tullius SG, Nieminen M, Bechstein WO, Jonas S, Steinmuller T, Qun Y, Pratschke J, Graser E, Sinha P, Volk HD, Neuhaus P, Tilney NL (1998) Contribution of early acute rejection episodes to chronic rejection in a rat kidney retransplantation model. *Kidney Int* 53(2):465–472. doi:10.1046/j.1523-1755.1998.00757.x

27. Grande MT, Sanchez-Laorden B, Lopez-Blau C, De Frutos CA, Boutet A, Arevalo M, Rowe RG, Weiss SJ, Lopez-Novoa JM, Nieto MA (2015) Snail1-induced partial epithelial-to-mesenchymal transition drives renal fibrosis in mice and can be targeted to reverse established disease. *Nat Med* 21(9):989–997. doi:10.1038/nm.3901
28. Lin L LD, Liang H, Xue L, Su C, Liu M. (2015) MiR-1228 promotes breast cancer cell growth and metastasis through targeting SCAI protein. *Int J Clin Exp Pathol* 1 (8(6)):6646–6655
29. Lobry C, Oh P, Aifantis I (2011) Oncogenic and tumor suppressor functions of Notch in cancer: it's NOTCH what you think. *J Exp Med* 208(10):1931–1935. doi:10.1084/jem.20111855
30. Nozawa RS, Nagao K, Masuda HT, Iwasaki O, Hirota T, Nozaki N, Kimura H, Obuse C (2010) Human POGZ modulates dissociation of HP1alpha from mitotic chromosome arms through aurora B activation. *Nat Cell Biol* 12(7):719–727. doi:10.1038/ncb2075
31. Brauchle M, Yao Z, Arora R, Thigale S, Clay I, Inverardi B, Fletcher J, Taslimi P, Acker MG, Gerrits B, Voshol J, Bauer A, Schubeler D, Bouwmeester T, Ruffner H (2013) Protein complex interactor analysis and differential activity of KDM3 subfamily members towards H3K9 methylation. *PLoS One* 8(4):e60549. doi:10.1371/journal.pone.0060549
32. Moldovan GL, Pfander B, Jentsch S (2007) PCNA, the maestro of the replication fork. *Cell* 129(4):665–679. doi:10.1016/j.cell.2007.05.003
33. Mailand N, Gibbs-Seymour I, Bekker-Jensen S (2013) Regulation of PCNA-protein interactions for genome stability. *Nat Rev Mol Cell Biol* 14(5):269–282. doi:10.1038/nrm3562
34. Milutinovic S, Zhuang Q, Szyf M (2002) Proliferating cell nuclear antigen associates with histone deacetylase activity, integrating DNA replication and chromatin modification. *J Biol Chem* 277(23):20974–20978. doi:10.1074/jbc.M202504200
35. Murzina N, Verreault A, Laue E, Stillman B (1999) Heterochromatin dynamics in mouse cells. *Mol Cell* 4(4):529–540. doi:10.1016/s1097-2765(00)80204-x
36. Hansen RK, Mund A, Poulsen SL, Sandoval M, Klement K, Tsouroula K, Tollenaere MA, Raschle M, Soria R, Offermanns S, Worzfeld T, Grosse R, Brandt DT, Rozell B, Mann M, Cole F, Soutoglou E, Goodarzi AA, Daniel JA, Mailand N, Bekker-Jensen S (2016) SCAI promotes DNA double-strand break repair in distinct chromosomal contexts. *Nat Cell Biol*. doi:10.1038/ncb3436
37. Isobe SY, Nagao K, Nozaki N, Kimura H, Obuse C (2017) Inhibition of RIF1 by SCAI allows BRCA1-mediated repair. *Cell Rep* 20(2):297–307. doi:10.1016/j.celrep.2017.06.056
38. Bai F, Chan HL, Scott A, Smith MD, Fan C, Herschkowitz JI, Perou CM, Livingstone AS, Robbins DJ, Capobianco AJ, Pei XH (2014) BRCA1 suppresses epithelial-to-mesenchymal transition and stem cell dedifferentiation during mammary and tumor development. *Cancer Res* 74(21):6161–6172. doi:10.1158/0008-5472.CAN-14-1119